Lahouari Boukhris, Mostefa Bouchetara

RESEARCH ON BRAKE FORCES DISTRIBUTION IN A PASSENGER CAR

ISTRAŽIVANJE RASPODELE SILA KOČENJA U PUTNIČKOM AUTOMOBILU

Originalni naučni rad / Original scientific paper
UDK /UDC: 629.3-592

Rad primljen / Paper received: 29.07.2019

Adresa autora / Author's address:
Faculty of Mechanical Engineering, University of Sciences and Technology of Oran, Mohamed Boudiaf, Oran, Algeria
email: lahouari.boukhris@univ-usto.dz

Keywords
- brake force distribution
- distribution diagram
- friction coefficient

Abstract

Rapid growth of the fleet and development of road networks with high traffic are accompanied by a drastic increase in the number of accidents, despite the road safety companion. The braking system contributes greatly to the improvement of active safety. It should be characterized by its efficiency, escalation, fidelity and security. To achieve these criteria, a study is necessary of the distribution of braking forces in the braking system design phase, regardless of operating conditions and state of the road.

Ključne reči
- raspodela sila kočenja
- dijagram raspodele
- koeficijent trenja

Izvod

Nagli rast saobraćajne flote i razvoj putne mreže sa gustim saobraćajem prati drastičan porast broja nesreća, uprkos pratećim bezbednosnim faktorima. Sistem kočenja u velikoj meri doprinosi poboljšanju aktivne bezbednosti i treba da ga karakterišu efikasnost, raširenost, pouzdanost i bezbednost. Radi postizanja ovih kriterijuma, neophodna je studija o raspodeli sila kočenja u fazi projektovanja kočionog sistema, bez obzira na uslove rada i stanja puteva.

INTRODUCTION

Active safety of a vehicle is mainly influenced by properties of the installed braking system. With increase in road traffic density and travel speeds, increasingly stringent requirements are placed on the vehicle's behaviour during braking. The achievable decelerations are limited by the physical aspect characterized by the coefficient of friction between the tires and the ground. As a result, it follows that an optimized distribution of braking forces becomes necessary for a better use of friction coefficients. This objective could only be achieved if sufficient knowledge is available on the theory of vehicle dynamics during braking and on current standards for the approval of braking systems. These will facilitate the development of a braking force calculation algorithm that will enable an optimized distribution of braking forces to be achieved. Operating safety is conditioned by the requirements of efficiency, progressiveness, regularity or fidelity of a braking system, without obviously neglecting the recommendations imposed by the legislator.

EFFORTS APPLIED TO A VEHICLE DURING BRAKING

Efforts applied to a braked wheel

The wheel is the element that transmits braking torque to the ground and determines the direction of the vehicle. For any study of the braking system, the case of a braked wheel must be examined. Thus, factors influencing wheel behaviour and interactions between the wheel, vehicle connecting parts and the ground can be defined.

Between the wheel and the ground, there are two reaction forces, one vertical R_V and the other tangential R_B (Fig. 1). The thrust F_A applied to the wheel axis is in balance with the tangential resistance R_B which is equal to the sum of braking force F_B and the rolling resistance force,

$$F_A = F_B + F_R \,. \qquad (1)$$

The condition for having a bearing with wheel slip is

$$F_A = F_B + F_R \leq \mu_S F_G \,. \qquad (2)$$

By neglecting the rolling resistance ($F_R = 0$), the braking condition of the wheel becomes

$$F_B \leq \mu_S F_G \,. \qquad (3)$$

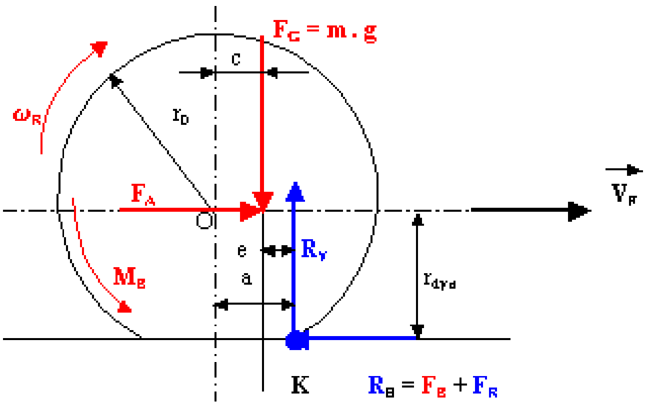

Figure 1. Forces acting on a braked wheel.

Adhesion varies with weight F_G and coefficient μ_S. The latter depends on the wheel tread, road conditions, and tyre inflation pressure /1-4/.

In the case of a braked wheel, the peripheral speed of the wheel V_R is smaller than the vehicle speed V. This speed difference is expressed by the slip coefficient, /1, 3, 4/:

$$s = \frac{V - V_R}{V} 100\% \,. \qquad (4)$$

It is obvious that with zero slip, there is no transmission of braking force on the ground; we have a pure wheel bearing. With a relatively small slip (s = 20 to 30 %), the braking force transmitted to the ground reaches its maximal value and corresponds to the grip force. From this point on, the braking efficiency decreases with increasing slip. The static friction coefficient μ_S becomes a dynamic sliding coefficient, /4/.

Efforts acting on a vehicle stopped on a flat surface

In the case of a stationary vehicle, most natural resistances have no effect. On a flat surface, the vehicle is not subjected to either natural or artificial resistance ($F_B = 0$); only the vertical reactions of the ground are present (Fig. 2).

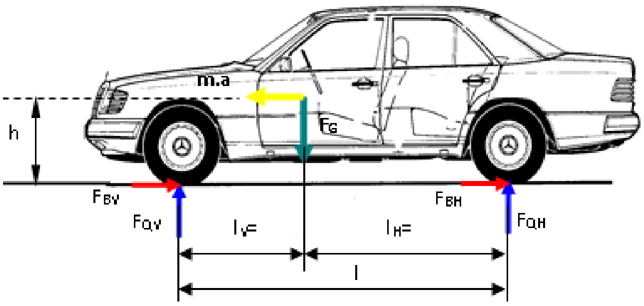

Figure 2. Efforts acting on a vehicle.

The general equation of braking forces is expressed as follows, /1-4/:

$$\frac{F_{BI}}{F_G} = \mu_S \eta \frac{F_{QI}}{F_G} . \tag{5}$$

Braking efficiency z is the ratio between deceleration a and gravity acceleration g; it is expressed as a percentage, /1-4/:

$$z = \frac{a}{g} 100\% . \tag{6}$$

By neglecting the natural resistances, it results from the balance of the horizontal forces of the vehicle with, or without a flat braked trailer,

$$z = \frac{\sum F_{Bi}}{\sum F_{Gj}} 100\% , \tag{7}$$

where: F_{Bi} - braking force acting on axle *'i'*; F_{Gj} - weight of each vehicle *'j'* of the coupling (in the case of a trailer).

For a two-axle vehicle without trailer, Eq.(7) takes the following form

$$z = \frac{F_{BV}}{F_G} + \frac{F_{BH}}{F_G} , \tag{8}$$

where: V - index corresponding to the front axle; H- index corresponding to the rear axle; F_G - weight of the vehicle.

Reflections made for the whole vehicle can be applied in a similar way for each axle. In regulation N°13, we define the coefficient of friction f, relative to the axle 'i', also called the specific braking force, /1-4/:

$$f_i = \frac{F_{Bi}}{F_{Qi}} , \tag{9}$$

$$f_i = \mu_S \eta_i , \tag{10}$$

where: F_{Qi} - the dynamic load applied to axle 'i'.

By replacing Eqs.(5) and (9) in Eq.(7), we obtain:

$$z = \sum f_i \frac{F_{Qi}}{F_{Gj}} = \mu_s \frac{\sum \eta_i F_{Qi}}{\sum F_{Gj}} . \tag{11}$$

From Eq.(10), the overall rate of adhesion utilization is derived:

$$\eta = \sum \eta_i \frac{F_{Qi}}{F_{Gj}} , \tag{12}$$

for a two-axle vehicle we have

$$\eta = \frac{z}{\mu_S} = \eta_V \frac{F_{QV}}{F_G} + \eta_H \frac{F_{QH}}{F_G} , \tag{13}$$

$$\frac{F_{QV}}{F_G} = \frac{l_H}{l} + \frac{h}{I} z , \tag{14}$$

$$\frac{F_{QH}}{F_G} = \frac{l_V}{l} - \frac{h}{I} z , \tag{15}$$

where: l_V - horizontal distance from the centre of gravity to the front axle; l_H - horizontal distance from the centre of gravity to the rear axle; h - height of the centre of gravity above the ground.

VEHICLE BRAKING EVALUATION VARIABLES

European regulation N°13 defines the different variables used to assess the braking and braking systems of vehicles. The control provisions of the braking systems refer to a vehicle braked on a plane, neglecting natural resistances. Figure 2 shows a calculation model for a car without a trailer under these conditions. The most important variable that characterizes the effectiveness of a vehicle's braking system is the braking distance. It depends on the initial speed, maximum deceleration and actual braking time /5-8/.

Braking forces for two-axle vehicles

Applying Eqs.(5) and (10) to two-axle vehicles gives the following expressions:

$$\frac{F_{BV}}{F_G} = f_V \left(\frac{l_H}{l} + \frac{h}{I} z \right) = \eta_V \mu_V \left(\frac{l_H}{l} + \frac{h}{I} z \right), \tag{16}$$

$$\frac{F_{BH}}{F_G} = f_H \left(\frac{l_V}{l} + \frac{h}{I} z \right) = \eta_H \mu_H \left(\frac{l_V}{l} + \frac{h}{I} z \right), \tag{17}$$

with $f_V \le \mu_V$ and $f_H \le \mu_H$.

In European standards N°13 only one adhesion coefficient $\mu_V = \mu_H = \mu_S$ /4/ is considered. By removing μ_V, μ_H and z from Eqs.(16) and (17), we obtain an equation that is valid for all braking situations of a vehicle running on a flat surface:

$$\left(\frac{F_{BV}}{F_G} \right)^2 - \frac{F_{BV}}{F_G} + \frac{l_V}{h} + \frac{F_{BV}}{F_G} \frac{F_{BH}}{F_G} \frac{\eta_V + x\eta_H}{x\eta_H} + \\ + \frac{F_{BH}}{F_G} \frac{\eta_V}{x\eta_H} \frac{l_H}{h} + \frac{\eta_V}{x\eta_H} \left(\frac{F_{BH}}{F_G} \right)^2 = 0 , \tag{18}$$

with $x = \frac{\mu_H}{\mu_V}$ and $\frac{l_V}{l} + \frac{l_H}{l} = 1$.

Equation (18) represents a parabola, whose inflection point is not confused with the origin of the coordinates and whose axis of symmetry forms an angle of 135° with respect to the positive abscissa, /5-8/. The braking force distribution diagram (DREF) to be commented on contains this type of parabola of the shape $\frac{F_{BH}}{F_G} = f\left(\frac{F_{BV}}{F_G}\right)$.

Ideal distribution of braking forces in a two-axle vehicle

From the above equations, any braking state can be studied; it is sufficient to know the conditions at the corresponding limits. The ideal or theoretical distribution is characterized by the fact that all the wheels are simultaneously at the beginning of the lock. The coefficient of friction during braking equals unity ($\eta = 1$). The boundary conditions for the ideal distribution are as follows, /1-4/:

$$\left.\begin{aligned} & f_V = f_H = \mu_V = \mu_H = \mu_S = z \\ & \eta_V = \eta_H = 1.0 \ , \ \ x = 1.0 \end{aligned}\right\} \tag{19}$$

The explicit form of the function $\frac{F_{BH}}{F_G} = f\left(\frac{F_{BV}}{F_G}\right)$ for an ideal distribution is written as follows:

$$\frac{F_{BH}}{F_G} = -\frac{l_H}{2h} - \frac{F_{BV}}{F_G} \pm \sqrt{\left(\frac{l_H}{2h}\right)^2 + \frac{F_{BV}}{F_G}\frac{l}{h}} \ . \tag{20}$$

This relationship is only valid for the conditions imposed in European regulations.

For the chosen example, the numerical application gives the following function of the ideal distribution curve with $\eta_V = \eta_H = 1$:

$$\frac{F_{BH}}{F_G} = -\frac{1}{2 \cdot 0.5} - \frac{F_{BV}}{F_G} \pm \sqrt{\left(\frac{1}{2 \cdot 0.5}\right)^2 + \frac{F_{BV}}{F_G}\frac{2.5}{0.5}} \ . \tag{21}$$

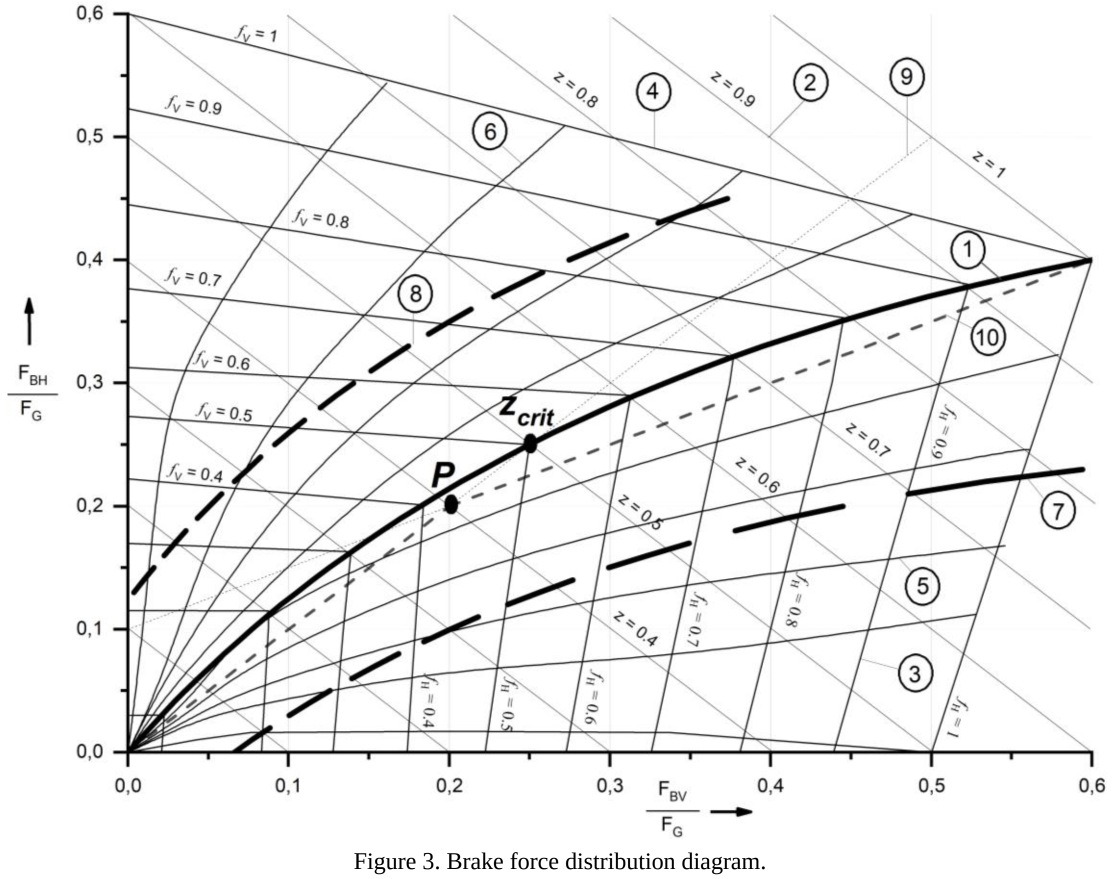

Figure 3. Brake force distribution diagram.

In the diagram in Fig. 3, the curve (1) represents the pace of the ideal distribution of braking forces. Due to its parabolic appearance, the ideal distribution cannot be achieved with reasonable technical means. The actual or installed brake force distribution has a linear or broken linear characteristic. In addition, it is not recommended to have all wheels locked simultaneously during an emergency brake application. Figure 3 shows other straight lines and curves, which are of great importance for the construction and evaluation of braking systems. The lines (2) represent constant efficiency curves (z = *constant*). In the range between the axle F_{BV}/F_G and the ideal distribution curve, there is a locking of the front wheels and then the rear wheels and vice versa in the range between the axle F_{BH}/F_G and the ideal distribution curve. These two braking states will be analysed in the section below.

Not ideal distribution of braking forces

– Distribution of braking forces with constant f_V or f_H

a) f_V = *constant*

All curves with f_V = *constant* intersect at a point on the negative part of the axis F_{BH}/F_G corresponding to $F_{BH}/F_G = -l_H/h$. In the range between the ideal distribution curve and the axis F_{BH}/F_G, there is a locking of the rear wheels before the front wheels

b) f_H = *constant*

All lines with f_H = *constant* meet at a point on the positive side of the axis F_{BV}/F_G, whose value is equal to l_V/l. Figure 3 shows that the lines 4 with f_V = *constant* or the lines 3 with f_H = *constant* intersect on the ideal distribution curve which represents the geometric location of the intersection points of the lines with f_I constant. When the friction coefficients of the front and rear wheels are not equal, the straight lines with f_I = *constant* remain the same, but their intersection points are no longer on the ideal distribution curve.

– Brake force distribution with η = *constant*

The adhesion utilization rate η does not give any information on the blocking order. A grip utilization rate $\eta < 1$ can be achieved with both front and rear wheel locking risk.

a) η = *constant* with risk of locking the front wheels ($f_V = \mu$ and $z = \eta\mu$)

By taking η = *constant*, we can determine the curves 5 in Fig. 3, whose explicit relationship is as follows:

$$\frac{F_{BH}}{F_G}=-\frac{l_H}{2h}-\frac{F_{BV}}{F_G}\pm\sqrt{\left(\frac{l_H}{2h}\right)^2+\eta\frac{l}{h}\frac{F_{BV}}{F_G}}\ . \qquad (22)$$

b) $\eta_V = 1$ and $\eta_H < 1$, with risk of locking the front wheels ($f_V = \mu_V$ and $f_H < \mu_H \rightarrow z < z_{id}$)

The braking forces for this case are as follows:

$$\left.\begin{aligned}\frac{F_{BV}}{F_G}&=\mu_V\left(\frac{l_H}{l}-\frac{h}{l}z\right)\\ \frac{F_{BH}}{F_G}&=\eta_H\,\mu_H\left(\frac{l_H}{l}+\frac{h}{l}z\right)\end{aligned}\right\} \qquad (23)$$

c) η = *constant*, with risk of rear wheel locking ($f_H = \mu_S\cdot\eta$ = *constant*, $z = \mu_S\cdot\eta$)

From Eqs.(16) and (17), it follows:

$$\left.\begin{aligned}\frac{F_{BV}}{F_G}&=f_V\left(\frac{l_H}{l}-\frac{h}{l}\eta\mu_S\right)\\ \frac{F_{BH}}{F_G}&=\mu_S\left(\frac{l_V}{l}+\frac{h}{l}\eta\mu_S\right)\end{aligned}\right\} \qquad (24)$$

For η = *constant* we obtain the curves 6 shown in Fig. 3.

Braking forces with minimum efficiencies according to ECE R 13 regulation

– Distribution of braking forces with a risk of locking the front wheels ($f_v = \mu_S$)

Now we must differentiate between wheel lock states in the case of minimum efficiencies set by European standards.

For the efficiency limit curves, we have:

$$\left.\begin{aligned}z_{ECE}&=A\mu_S-B\\ \frac{F_{BV}}{F_G}&=\mu_S\left[\frac{l_H}{l}-\frac{h}{l}(A\mu_S-B)\right]\\ \frac{F_{BH}}{F_G}&=\eta_H\,\mu_S\left[\frac{l_V}{l}+\frac{h}{l}(A\mu_S-B)\right]\end{aligned}\right\} \qquad (25)$$

With these equations, the minimum efficiency curve according to Regulation No.13 is plotted with the risk of locking the front wheels, Fig. 3.

– Distribution of braking forces with risk of rear wheel locking ($f_H = \mu_S$)

Braking forces with risk of locking the rear wheels are:

$$\left.\begin{aligned}\frac{F_{BV}}{F_G}&=f_V\left[\frac{l_V}{l}-\frac{h}{l}(A\mu_S-B)\right]\\ \frac{F_{BH}}{F_G}&=\mu_S\left[\frac{l_V}{l}-\frac{h}{l}(A\mu_S-B)\right]\end{aligned}\right\} \qquad (26)$$

Curve 8 in Fig. 3 shows the distribution of braking forces with a minimum efficiency according to Regulation No. 13 with a risk of locking the rear wheels. Curves 7 and 8 represent the upper and lower limits of the permissible braking range according to European standards respectively.

– Distribution of braking forces with minimum efficiency and risk of locking the front wheels ($f_V = \mu_V\cdot\eta_{ECE}$) and rear wheels ($f_H = \mu_H\cdot\eta_{ECE}$), respectively

In this case it is considered that $\mu_S = \mu_V$, since the friction coefficient μ_V of the front wheels is decisive. The calculation of braking forces with minimum efficiency z_{ECE} takes place in the range of $\mu_S = \mu_V$ = 0.2 to 0.8, i.e. $z_{ECE} = 0.85\cdot\mu_V - 0.07$. With this efficiency, the dynamic loads at the front and rear axles are calculated.

In the case of locking the front wheels, we have:

$$\left.\begin{aligned}\frac{F_{BV}}{F_G}&=\mu_{ECE}\frac{F_{BV}}{F_G}\\ \frac{F_{BH}}{F_G}&=z_{ECE}-\frac{F_{BV}}{F_G}\end{aligned}\right\} \qquad (27)$$

In the case of locking the rear wheels, we have:

$$\left.\begin{aligned}\frac{F_{BH}}{F_G}&=\mu_{ECE}\frac{F_{BV}}{F_G}\\ \frac{F_{BV}}{F_G}&=z_{ECE}-\frac{F_{BH}}{F_G}\\ \mu_H&=x\mu_V \quad \text{and} \quad x>1\end{aligned}\right\} \qquad (28)$$

For vehicles of category M1, the locking of the rear wheels before the front wheels is allowed in the range of z = 0.30 to z = 0.45, if the curve $\frac{F_{BH}}{F_G}=f\left(\frac{F_{BV}}{F_G}\right)$ with $f_H = \mu_H$ of the rear wheels does not exceed the ideal curve of 0.05. In the range z = 0.30 … 0.45 an ideal curve $\mu_S = \mu_V = \mu_H = z$ for $\mu_S = z + 0.05$ or $z = \mu_S - 0.05$ must be described to represent the realisation range of the braking system, /4/. This limit curve is determined in the same way as the z ECE curve with the risk of locking the rear wheels. In Regulation No. 13, it is permitted that the rear wheels be braked before the front wheels, but not exceeding the curve corresponding to $z = \mu_S - 0.05$, /4/. Referring to the diagram in Fig. 3, the range of the actual brake force distribution is between curve 1 and the ideal distribution and curve 7 with $\eta = \eta_{ECE}$ and front wheels locking.

ACTUAL DISTRIBUTION OF BRAKING FORCES

Unlike the limit braking conditions examined, the actual distribution of braking forces is now being investigated. Assuming that there is a linear relationship between the pressure exerted on the brake and the braking moment at the wheel. This results in a linear correlation between the front and rear braking forces, represented in the braking force distribution diagram by a line from the origin, such as line 9 in Fig. 3, where it is generally accepted that the wheels of an axle lock when the curve of the installed brake force distribution intersects the respective lines with real friction coefficient f_I = *constant*. If the first intersection point is below the ideal distribution curve, then the front wheels lock in front of the rear wheels; if it is above, the rear wheels lock in first. Figure 3 shows these two situations. With line 9, we have a locking of the front wheels up to point *P*. With the line 10 it is from point *P*.

An important characteristic variable is the critical efficiency z_{crit}, which corresponds to the intersection point of the actual distribution and the ideal distribution, /5-8/:

$$z_{crit} = \frac{1}{h}\left[\frac{F_{BH}}{\mu_H} - \frac{1}{1+\left(\frac{F_{BV}}{F_{BH}}\right)_{inst}}\right]. \tag{29}$$

According to European Regulation No. 13, the critical efficiency z_{crit} must be greater than 0.82. Experience shows that it is advantageous to choose z_{crit} between 0.9 and 1.0, /4/. When the driver acts on the brake pedal, the front and rear braking force increase along the installed distribution line until it intersects the permissible line with a constant actual friction coefficient (f_V = *constant*).

CONCLUSION

After presenting the theoretical basis on vehicle dynamics for determining the braking forces applied to the front and rear wheels, it is shown that the coefficient of friction during braking has a major influence on the construction of the braking system. The increase in the friction coefficient of the rear wheels compared to the front wheels has a positive effect on braking efficiency.

The current method of designing and controlling braking systems is incomplete, as it considers that the friction coefficient of the front and rear wheels are the same.

The brake force distribution curve must be within the range prescribed by the regulations in force, which is between the ideal distribution curve and the minimum efficiency curve. This requires high friction coefficients during braking. This is possible if the tyre load and inflation pressure are within the permissible range. On the ideal distribution curve, all the wheels of the vehicle are at the same time at the beginning of the lock. A linear distribution only reaches this state at the critical point. With the algorithm developed, it is possible to plot curves representing the relationship between the braking effort exerted on the pedal, the braking pressure on the front and rear brakes, and the braking efficiency of the braking system. To avoid the risk of locking the front rear wheels before the front wheels, there are currently brake pressure limiting devices for the rear brakes, /1, 3, 4/.

REFERENCES

1. Stone, R., Ball, J.K., Automotive Engineering Fundamentals, SAE Int., 2004.
2. Balkwill, J., Performance Vehicle Dynamics, Engineering and Applications, Butterworth-Heinemann, 2018.
3. Day, A., Braking of Road Vehicles, Butterworth-Heinemann, 2014.
4. Gillespie, T.D., Fundamentals of Vehicle Dynamics, SAE Int., 1992.
5. Peng, H., Hu, J.-S. (1996), *Traction/braking force distribution for optimal longitudinal motion during curve following*, Veh. System Dynam. 26(4):301-320. doi: 10.1080/00423119608969313
6. Zhang, H., Cao, D., Du, H. (Eds.), Modeling, Dynamics and Control of Electrified Vehicles, Woodhead Publishing, 2018. doi: 10.1016/C2016-0-03862-7
7. Li, C., Li, X., Zhou, W., Dai, W. (2014), *Theoretical research on ideal brake force distribution of tractor-semitrailer cornering braking*, Appl. Mech. Mater. 467: 451-455. doi: 10.4028/www.scientific.net/AMM.467.451
8. Nakazawa, M., Isobe, O., Takahashi S., Watanabe, Y. (1995), *Braking force distribution control for improved vehicle dynamics and brake performance*, Vehicle Syst. Dyn.: Int. J Veh. Mech. Mobility, 24(4-5): 413-426. doi: 10.1080/00423119508969101

© 2019 The Author. Structural Integrity and Life, Published by DIVK (The Society for Structural Integrity and Life 'Prof. Dr Stojan Sedmak') (http://divk.inovacionicentar.rs/ivk/home.html). This is an open access article distributed under the terms and conditions of the Creative Commons Attribution-NonCommercial-NoDerivatives 4.0 International License